

# Somatic Mutation of *p53* Leads to Estrogen Receptor $\alpha$ -Positive and -Negative Mouse Mammary Tumors with High Frequency of Metastasis

Suh-Chin J. Lin,<sup>1,2</sup> Kuo-Fen Lee,<sup>4</sup> Alexander Yu. Nikitin,<sup>5</sup> Susan G. Hilsenbeck,<sup>6</sup> Robert D. Cardiff,<sup>7</sup> Aihua Li,<sup>1,2</sup> Keon-Wook Kang,<sup>1,2</sup> Steven A. Frank,<sup>3</sup> Wen-Hwa Lee,<sup>2</sup> and Eva Y-H. P. Lee<sup>1,2</sup>

<sup>1</sup>Departments of Developmental and Cell Biology, <sup>2</sup>Biological Chemistry, and <sup>3</sup>Ecology and Evolutionary Biology, University of California, Irvine, California; <sup>4</sup>The Salk Institute for Biological Studies, La Jolla, California; <sup>5</sup>Department of Biomedical Sciences, Cornell University, Ithaca, New York; <sup>6</sup>Department of Medicine and Department of Molecular and Cellular Biology, Breast Center, Baylor College of Medicine, Houston, Texas; and <sup>7</sup>Center for Comparative Medicine, University of California, Davis, California

## ABSTRACT

Approximately 70% of human breast cancers are estrogen receptor  $\alpha$  (ER $\alpha$ )-positive, but the origins of ER $\alpha$ -positive and -negative tumors remain unclear. Hormonal regulation of mammary gland development in mice is similar to that in humans; however, most mouse models produce only ER $\alpha$ -negative tumors. In addition, these mouse tumors metastasize at a low rate relative to human breast tumors. We report here that somatic mutations of *p53* in mouse mammary epithelial cells using the Cre/loxP system leads to ER $\alpha$ -positive and -negative tumors. *p53* inactivation under a constitutive active *WAPCre<sup>c</sup>* in prepubertal/pubertal mice, but not under *MMTVCre* in adult mice, leads to the development of ER $\alpha$ -positive tumors, suggesting that target cells or developmental stages can determine ER $\alpha$  status in mammary tumors. Importantly, these tumors have a high rate of metastasis. An inverse relationship between the number of targeted cells and median tumor latency was also observed. Median tumor latency reaches a plateau when targeted cell numbers exceed 20%, implying the existence of saturation kinetics for breast carcinogenesis. Genetic alterations commonly observed in human breast cancer including *c-myc* amplification and Her2/Neu/erbB2 activation were seen in these mouse tumors. Thus, this tumor system reproduces many important features of human breast cancer and provides tools for the study of the origins of ER $\alpha$ -positive and -negative breast tumors in mice.

## INTRODUCTION

Breast carcinogenesis requires multiple genetic changes including inactivation of tumor suppressor genes and activation of oncogenes (1). Mutations in *p53* are observed in close to half of human cancers including breast carcinomas (2). *p53* is also mutated in families with Li-Fraumeni syndrome in which early-onset female breast cancer is the most prevalent type of tumor (3). *p53* is a transcription factor that regulates genes critical for cell cycle arrest and for apoptosis after genotoxic stress, thus preventing genome instability (4–6). In addition, amplification and/or overexpression of *c-myc*, *Her2/Neu/erbB2*, and *cyclin D1* oncogenes are seen in a significant portion of breast cancers (2, 7).

*p53* knockout mice are cancer prone and develop early-onset lymphoma and sarcoma (8, 9) but rarely mammary tumors (10) because of early mortality. To circumvent this problem, *p53<sup>null</sup>* mammary epithelium is transplanted into the fat pad of wild-type recipients and leads to the formation of breast tumors (11). Although this offers a potential model to study breast tumors, the influence of the transplantation process on carcinogenesis is not clear. Also, the transplanted cells are *p53<sup>null</sup>*, whereas in human tumors somatic mutations are acquired in a subset of cells during tumor progression. Previously, Jonkers *et al.* (12) reported that no mammary tumor formation was observed in *p53* conditional-mutant mice carrying K14Cre transgene. Therefore, conditional inactivation

of *p53* in mouse mammary epithelial cells is necessary to generate a mouse model mimicking human carcinogenesis.

In addition to genetic mutations, steroid hormones play a critical role in breast carcinogenesis (13). About 70% of human breast cancers are estrogen receptor  $\alpha$  (ER $\alpha$ )-positive and estrogen-dependent (14), and ER $\alpha$  and progesterone receptor (PR) expression is an important indicator of potential responses to hormonal therapy (15). However, the factors that control ER $\alpha$  expression in tumor cells are unknown. Thus far, most established mouse models seldom produce ER $\alpha$ -positive mammary tumors (16). In a C3(1)/SV40 T-antigen-transgenic model, ER $\alpha$  expression decreases during early mammary tumor progression (from low- to high-grade mammary intraepithelial neoplasia and becomes undetectable in invasive tumors (17). In *Brca1*- and *Brca2*-linked mammary tumors, the majority of tumors show no detectable ER $\alpha$  expression (18–20).

In humans, breast cancers frequently metastasize to other organs such as liver, lung, and specifically bone (21). Metastasis rather than primary tumors are responsible for most cancer mortality (21, 22). Less than 5% of patients with metastatic breast cancer have a long-term remission after treatment (22). In established mouse mammary tumor models, the tumor cells infrequently colonize other organs. Only 10% *Brca1* tumors (18), 10% *pten<sup>+/-</sup>* tumors (23), and 0% *Brca2* tumors (12, 20) metastasize. Many mouse mammary tumor virus (MMTV)/oncogene-bearing transgenic mice have a rare occurrence of metastasis (24), but metastatic tumors are observed in polyomavirus middle T antigen and neu proto-oncogene transgenic mice (25, 26).

We have generated a mouse breast tumor model by using Cre/loxP method to specifically inactivate *p53* in mammary epithelial cells. This conditional inactivation of *p53* leads to ER $\alpha$ -positive and -negative mammary tumors with a high rate of metastasis. We found that *p53* inactivation during specific developmental stages critically determines ER $\alpha$  expression in mammary tumors. This breast tumor system provides a close model of the human disease and will be useful for both mechanistic and therapeutic studies of ER $\alpha$ -positive breast cancer.

## MATERIALS AND METHODS

**Targeting Vector Construction.** A 10.75-kb clone covering exons 1–10 of *p53* was isolated from a 129sv mouse genomic library. The 3.4-kb *XhoI*-*HindIII* fragment containing exons 2–9 was subcloned into *pBR322*. A replacement-type targeting vector was made by inserting the first *loxP* site into a *BamHI* site located in intron 6. A *neo*-cassette flanked by two *loxP* sites was inserted into the *PvuII* site in intron 4. The resulting construct was cleaved with *XhoI* and *HindIII*, blunt-ended and subcloned into *p2TK* (27). The finished targeting construct is designated *p53neoloxp<sup>3</sup>2TK*.

**MMTVCre Transgene Construction.** The backbone of the *MMTVCre* transgene is *pBSpKCR3* (28) containing part of the rabbit  $\beta$ -globin gene (the end of exon 2, intron 2, and exon 3), and the polyadenylation site. A 1.6-kb *BglIII*-*HindIII* fragment composed of the *Cre* transgene with a nuclear localization signal was inserted within exon 3 of the *globin* gene of *pBSpKCR3*. A 1.5-kb *HindIII*-*NheI* fragment containing the *MMTV-LTR* was cut from *pMAM* (Clontech, Palo Alto, California) and subcloned 5' to exon 2 of the *globin* gene. The finished transgene construct is designated *pMMTV $\beta$ Cre*.

**MMTVCre-Transgenic Mice Production.** The 4.3-kb *XhoI* fragment containing the *MMTVCre* transgene was excised and purified. The transgenic

Received 11/10/03; revised 1/28/04; accepted 3/2/04.

**Grant support:** National Cancer Institute mouse consortium Grant CA04964, DOD BC013020, NIH CA84241, Breast Cancer Research Foundation to E. Lee and NCIP30 CA93373 to R. Cardiff.

The costs of publication of this article were defrayed in part by the payment of page charges. This article must therefore be hereby marked *advertisement* in accordance with 18 U.S.C. Section 1734 solely to indicate this fact.

**Requests for reprints:** Eva Y-H. P. Lee, University of California-Irvine, Sprague Hall, Room 140, 839 Health Science Court, Irvine, CA 92697-4037. Phone: (949) 824-9766; Fax: (949) 824-9767; E-mail: elee@uci.edu.

founders were generated by microinjecting the *MMTVCre* transgene fragment into the male pronucleus of fertilized eggs derived from CB6F1  $\times$  C57BL/6 intercrosses. Transgenic founders were identified by Southern analysis or PCR of tail DNA. The primers for the *Cre* transgene (363-bp amplified) were CreF (5'-GGTGTCCAATTTACTGACCGTACA-3') and CreR (5'-CGGATCCGC-CGCATAACCAGTG-3'). All mice were maintained in accordance with the guidelines of Laboratory Animal Research of The University of Texas Health Science Center at San Antonio and Institutional Animal Care and Use Committee of University of California, Irvine.

**Generation of Conditional *p53* Mutant Mice.** J1 embryonic stem cells were electroporated with *Sall*-linearized *p53<sup>neoloxp3</sup>2TK* and selected with G418 and 1-(2-deoxy-2-fluoro- $\beta$ -D-arabinofuranosyl)-5-iodouracil. Embryonic stem cells harboring homologous recombination were identified by Southern blotting using a 3' probe external to the targeting region. The *neo*-cassette was removed from targeted embryonic stem cells by transient expression of *pSPCre*. Of 231 clones analyzed by Southern blotting, two contained a recombination that removed only *neo*. These two clones were expanded and injected into C57BL/6 blastocysts. Chimeric males were mated with C57BL/6 females, and germline transmission of the mutant allele was verified by Southern and PCR analyses. Subsequently, *p53<sup>fp/fp</sup>MMTVCre* mice were generated by crossing *p53<sup>fp/fp</sup>* mice with *MMTVCre* mice. For PCR analysis, the following primers were used: primer x (5'-TGGGACAGCCAAGTCTGTGA-3'); y (5'-GCTGCAGGTCACCTGTAG-3'); z (5'-CATGCAGGAGCTATTACACA-3'); and p (5'-TACTCTCTCCCTCAATAAGTAT-3'). Primers "y" and "z" flank the *loxP* site in intron 6 and amplify a 119-bp fragment from wild-type *p53* and 158 bp from the *FP* allele. Primer pair x/z amplifies a ~500-bp fragment from the deleted allele after Cre-mediated recombination. Primer pair p/q amplifies a 327-bp product in the wild-type allele as well as a 253-bp fragment for the pseudogene.

*In vivo* functional analysis of Cre recombinase in double-transgenic mice carrying *Cre* and *R26R* reporter transgenes. To evaluate Cre activity *in vivo*, *Cre* mice were crossed with the *Rosa 26 reporter (R26R)* strain (29). Mammary glands from double-transgenic *Cre*; *R26R* mice were collected at different developmental stages and stained with X-gal for lacZ expression (30).

**Histology and Immunohistochemistry.** Collected tissues were fixed in 4% paraformaldehyde and processed through paraffin embedding following standard procedures. Sections were stained with H&E for histopathological evaluation. Immunostaining was performed following the protocol described in the Vectastain Elite ABC kit (Vector Laboratories, Burlingame, CA). For antigen retrieval, slides were heated for 20 min in 10 mM citrate buffer (pH 6.0) in a microwave oven. The antibodies used were CK8 and CK14 (1:2,000 and 1:300; The Binding Site, Birmingham, United Kingdom), ER $\alpha$  (1:2,000, MC-20; Santa Cruz Biotechnology, Santa Cruz, CA), PR and Neu/erbB2 (1:500 and 1:2,000; DAKO, Carpinteria, CA), and p53 (1:2,000, CM5; Novocastra Laboratories, Newcastle, United Kingdom).

**Western Analysis and Fluorescence Microscopy.** Tumor cells were grown in DMEM/F12 medium containing 15% fetal bovine serum, 10 ng/ml epidermal growth factor, and 1  $\mu$ g/ml insulin. Cell lysates were prepared using EBC (50mM Tris-HCl, 120 mM NaCl, 1 mM EDTA, pH 8.0, 50 mM NaF, 0.5% NP-40) buffer, and lysates (50  $\mu$ g) were separated by 10% gel electrophoresis and electrophoretically transferred to nitrocellulose paper. The nitrocellulose paper was incubated with anti-ER $\alpha$  (1:1,000, MC-20; Santa Cruz Biotechnology), anti-ER $\beta$  (1:1,000, PA1-311; Affinity Bioreagents, Golden, CO) or anti-actin (1:20,000; Sigma, St. Louis, MO) antibodies, followed by incubation with horseradish peroxidase or alkaline phosphatase-conjugated secondary antibodies, and developed using an enhanced chemiluminescence (ECL) or 5-bromo-4-chloro-3-indolyl phosphate/nitroblue tetrazolium solution. Tumor cells were infected with Ad-25ERE-GFP adenoviruses at a multiplicity of infection of ~100. Cells were precultured in serum-free DMEM/F12 for 1 day and treated with 10 nM 17- $\beta$  estradiol. Green fluorescent protein fluorescence was detected 24 h after 17- $\beta$  estradiol treatment.

## RESULTS

**Generation of the Floxed *p53* Allele.** We engineered the floxed *p53* allele (designated *p53<sup>fp</sup>*) by inserting the *loxP* sites into introns 4 and 6 of *p53* through a two-step process (Fig. 1, A and B). The phosphoglycerate kinase neomycin resistance cassette was subsequently removed by transient expression of Cre recombinase. Deletion

of exons 5 and 6 led to an in-frame deletion of 99 codons (codons 123–221) that encode part of the DNA-binding domain. The presence of *loxP* sites in introns 4 and 6 did not interfere with the transcription of *p53*, and the full-length p53 protein was detected in *p53<sup>fp/fp</sup>* mouse embryonic fibroblasts in the absence of Cre recombinase (Fig. 1C). A smaller protein product of expected mass of 39 kDa, designated *p53<sup>Δ5,6</sup>*, was detected in *p53<sup>fp/fp</sup>* mouse embryonic fibroblasts infected with Cre adenoviruses (Fig. 1C). IR-induced responses demonstrate that *p53<sup>Δ5,6</sup>* is transcriptionally inactive and fails to increase p21 target gene transcription. In contrast to wild-type p53, mutant *p53<sup>Δ5,6</sup>* protein was not stabilized after IR (Fig. 1D). No p53 protein was detected from mouse embryonic fibroblasts derived from *p53-null* (*p53<sup>-/-</sup>*) mice (Fig. 1, C and D).

**Characterization of Cre-Transgenic Mice.** To introduce somatic *p53* mutation in the mammary gland, different lines of mice expressing Cre under the control of MMTV-long terminal repeat, *MMTVCre<sup>a</sup>*, and *MMTVCre<sup>b</sup>* (collectively termed *MMTVCre*) were generated. In addition, to express Cre specifically in mammary luminal epithelial cells, *WAPrtACre*-transgenic mice in which Cre is regulated by the whey acidic protein (WAP) promoter were also used (31). In the *MMTVCre<sup>a</sup>* line, Cre activity was restricted to the mammary gland, whereas in *MMTVCre<sup>b</sup>* and *WAPrtACre* lines, Cre-mediated deletion was observed in many tissues (Fig. 2A). In contrast to the founder mice, when the *WAPrtACre* transgene was bred to floxed *p53* or reporter mice (see below), its activity became independent of doxycycline and pregnancy, likely attributable to modification of the transgene, and/or the unstable nature of the multicopy transgene. The altered transgene will be referred to as *WAPCre<sup>c</sup>* hereafter.

Because transgene activity varies depending on promoter and insertion sites, Cre-transgenic mice were crossed with *R26R* mice expressing LacZ after the removal of the floxed stop sequence by Cre (29) to identify the cell types targeted by Cre-mediated recombination in the mammary gland (Fig. 2B; Table 1; data not shown). In nulliparous *MMTVCre<sup>a</sup>*; *R26R* mice, LacZ was detected in ~0.7% cells of mammary gland. The expression remained low during 1st pregnancy and reached ~2.9% at 2nd pregnancy in both luminal epithelial and myoepithelial cells but not in stromal fibroblasts and adipocytes. In *MMTVCre<sup>b</sup>*; *R26R* mice, LacZ expression was also found in 5.6% of those cells in 2-week-old and ~20% in 7-week-old nulliparous mice. The expression increased to >60% in pregnant mice. The increased percentage of targeted cells in multiparous mice is expected, because MMTV promoter activities are up-regulated during pregnancy. In *WAPCre<sup>c</sup>*; *R26R* mice, LacZ activities were robust with 66% positive cells in 1-week-old and >90% in 17-day-old and 6-week-old nulliparous and pregnant mice. Thus, there are significantly higher numbers of targeted cells in *WAPCre<sup>c</sup>* than in *MMTVCre* mice during prepubertal/pubertal stages.

**Effects of *p53* Inactivation on Spontaneous Mammary Carcinogenesis.** As expected, these mice develop tumors with different spectrums. The most common tumor type is mammary tumor, and the majority of mammary tumor-bearing mice (60–80%) had multiple primary mammary tumors (Fig. 3; Table 2). Mammary tumor latency varied depending partly on numbers of targeted cells and parity of mice. Nulliparous *p53<sup>fp/fp</sup>MMTVCre<sup>a</sup>* females developed mammary tumors between 14 and 24 months of age with a median tumor latency (MTL) of 17.5 months with almost complete penetrance (23 of 24 mice), whereas all multiparous *p53<sup>fp/fp</sup>MMTVCre<sup>a</sup>* mice developed mammary tumors with a significantly shortened latency, between 11.5 and 24 months of age with a MTL of 15.5 months ( $P = 0.004$ , generalized Wilcoxon statistic). Both larger numbers of targeted cells as well as pregnancy-mediated cell proliferation could contribute to the shortened MTL. Nulliparous *p53<sup>fp/fp</sup>MMTVCre<sup>b</sup>* females developed mammary tumors between 6 and 14 months of age with a MTL of 10.5 months in nearly 50% of mice (9 of 19 mice), whereas

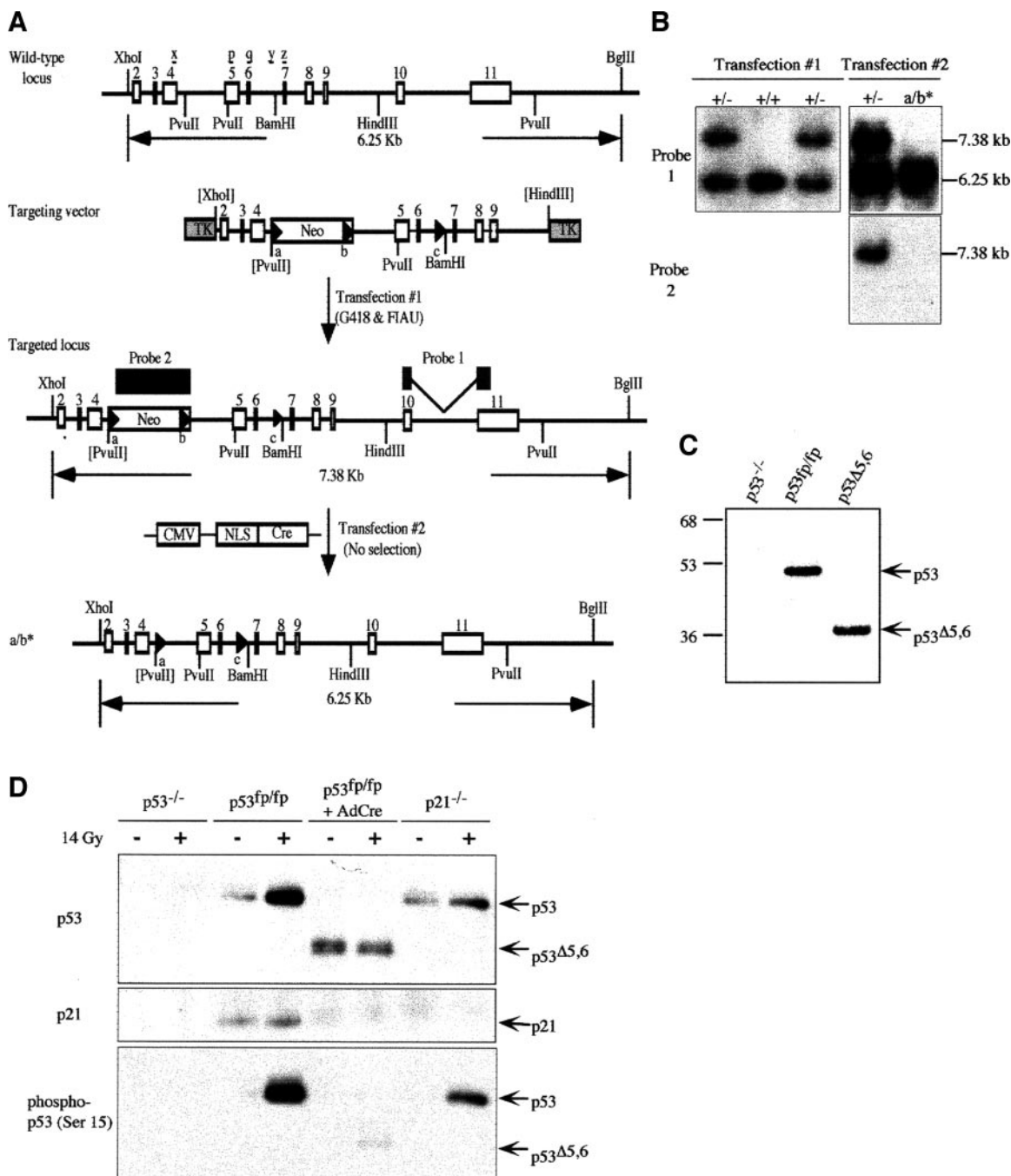


Fig. 1. Generation of conditionally inactivated *p53* alleles. **A**, maps of a portion of the wild-type *p53* locus, the targeting construct *p53<sup>neoloxp</sup>2TK*, the targeted *p53* locus, and the floxed *p53* allele (a/b\*). **B**, Southern analysis of embryonic stem clones. DNA was digested with *Xho*I plus *Bgl*II and hybridized with probe 1 containing exon 10 and part of exon 11 (top) or probe 2 containing *neo* sequence (bottom). Clone a/b\* carried a/b recombination, as shown by a 6.25-kb band when hybridized with probe 1 (top) and without signal when hybridized with probe 2 (bottom). The sizes of wild-type (6.25 kb) and targeted (7.38 kb) bands are also shown. **C**, Western analysis of p53 protein in mouse embryonic fibroblasts (MEFs). Expression of p53 protein in MEFs prepared from *p53*-null (*p53*<sup>-/-</sup>) mice and *p53*-floxed (*p53*<sup>fp/fp</sup>) mice, and in Cre adenoviruses infected *p53*<sup>fp/fp</sup> MEFs are shown. **D**, Western analysis of p53 protein levels (top), p21 induction (middle), and Ser-15 phosphorylation of p53 (bottom) in MEFs treated with 14Gy IR. FIAU, 1-(2-deoxy-2-fluoro- $\beta$ -D-arabinofuranosyl)-5-iodouracil; TK, thymidine kinase; CMV, cytomegalovirus; NLS, nuclear localization signal.

multiparous *p53*<sup>fp/fp</sup>*MMTVCre*<sup>b</sup> mice developed mammary tumors between 7 and 12 months of age with a MTL of 11 months in 60% of mice (12 of 20 mice). The MTL of *p53*<sup>fp/fp</sup>*MMTVCre*<sup>b</sup> mice is significantly shorter than that of *p53*<sup>fp/fp</sup>*MMTVCre*<sup>a</sup> mice ( $P < 0.001$ ), indicating distinct mammary carcinogenesis kinetics in mice with 1 or 3% versus  $\geq 20\%$  of *p53*-mutated cells. However, there is no statistical difference in the median MTL between 20% targeted cells in nulliparous and 60% in multiparous *p53*<sup>fp/fp</sup>*MMTVCre*<sup>b</sup> mice ( $P = 0.29$ ). The lower penetrance of mammary tumors in

*p53*<sup>fp/fp</sup>*MMTVCre*<sup>b</sup> was attributable to the presence of other tumor types leading to early death. In *p53*<sup>fp/fp</sup>*WAPCre*<sup>c</sup> mice, mammary tumors developed between 8 and 12.5 months of age with a MTL of 9.5 months with high penetrance (13 of 14 mice). Consistent with the findings in *p53*<sup>fp/fp</sup>*MMTVCre*<sup>b</sup>, increasing targeted cells to  $>90\%$  did not shorten the MTL further ( $P = 0.29$ ). Of note, only one 23.5-month-old multiparous heterozygous *p53*<sup>+/fp</sup>*MMTVCre*<sup>a</sup> mouse developed palpable mammary tumor in a cohort of mice between 20 and 26 months of ages ( $n = 12$ ; data not shown). The apparent long tumor

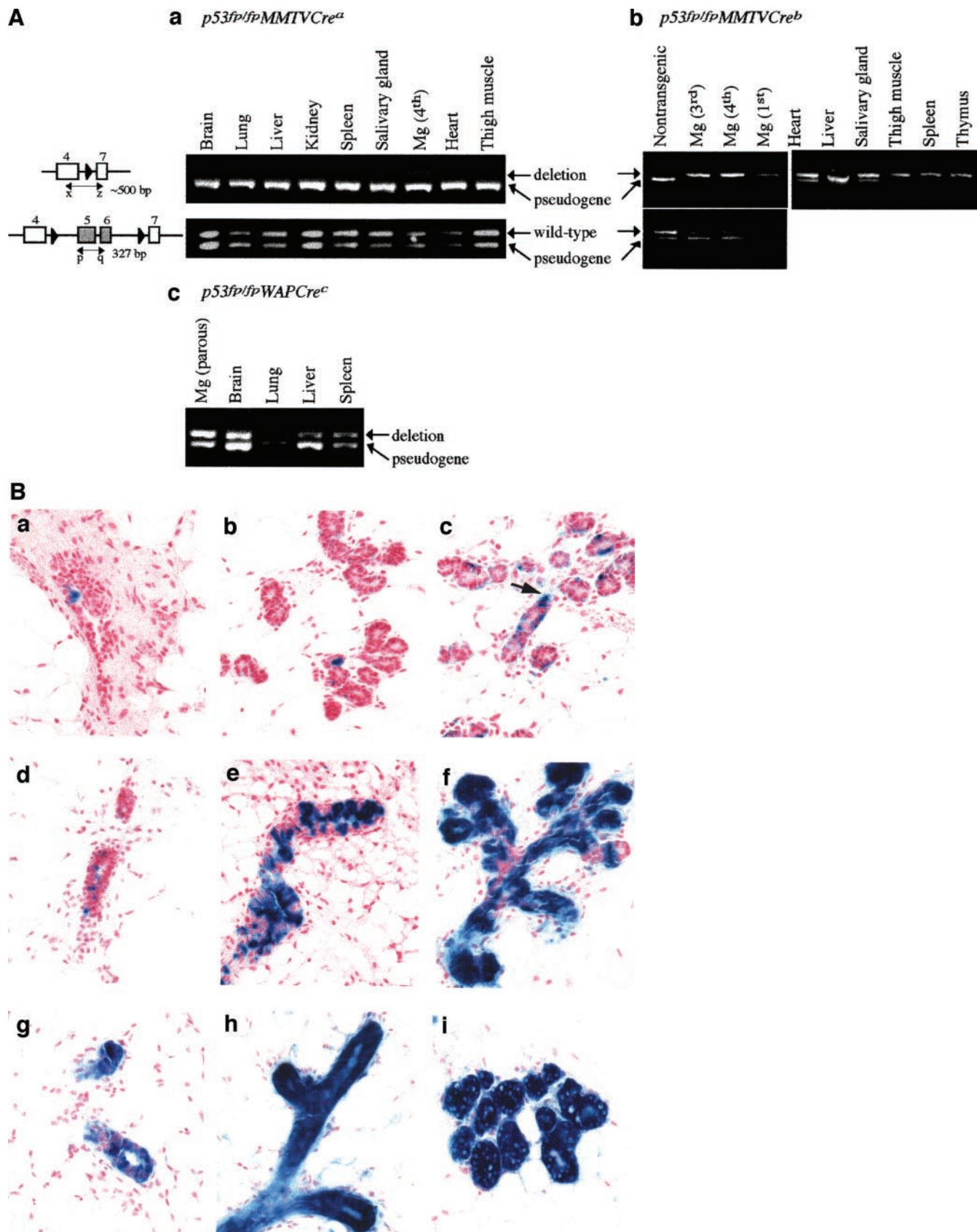


Fig. 2. Characterization of Cre activity. A, PCR analysis of Cre-mediated excision of floxed *p53* alleles in *p53<sup>flp/flp</sup>; Cre* mice. Primer pair x/z amplified a ~500-bp product in the deleted allele and a 377-bp fragment for the pseudogene, and primer pair p/q amplified a 327-bp product in the wild-type allele as well as a 253-bp fragment for the pseudogene. Tissue DNA samples were derived from *p53<sup>flp/flp</sup>MMTVCre<sup>a</sup>* (a), *p53<sup>flp/flp</sup>MMTVCre<sup>b</sup>* (b), and *p53<sup>flp/flp</sup>WAPCre<sup>c</sup>* (c) mice. Nontransgenic, non-Cre-transgenic mammary gland; Mg (1st), (3rd), (4th), and (parous), mammary gland of 1st, 3rd, 4th pregnancy and of a parous female. B,  $\beta$ -galactosidase staining of cells in the mammary gland of *Cre; R26R* mice. a-c, mammary gland from *MMTVCre<sup>a</sup>; R26R* mice, nulliparous (a), 1st pregnancy (b), 2nd pregnancy (c). Arrow in c indicates  $\beta$ -galactosidase detection in a myoepithelial cell; d-f, mammary gland from *MMTVCre<sup>b</sup>; R26R* mice, 2-week-old (d), nulliparous (e), 1st pregnancy (f); g-i, mammary gland from *WAPrtTACre; R26R* mice, 1-week-old (g), nulliparous (e), 1st pregnancy (f). Counterstained with nuclear fast red. Original magnifications,  $\times 200$ .

Table 1 *Cre*-mediated recombination in *Cre*; *R26R* mice

<i>Cre</i> transgene	Nulliparous/ pregnant	Site	X-gal positive cells (%) (mean $\pm$ SE) <sup>a</sup>
<i>MMTVCre<sup>a</sup></i>	Nulliparous (d42)	End bud/duct	0.73 $\pm$ 0.37 (n = 12)
	1st pregnancy	Alveoli	0.22 $\pm$ 0.12 (n = 12)
	2nd pregnancy	Alveoli	2.85 $\pm$ 0.44 (n = 12)
<i>MMTVCre<sup>b</sup></i>	Nulliparous (d50)	End bud/duct	18.97 $\pm$ 3.19 (n = 12)
	1st pregnancy	Alveoli	56.71 $\pm$ 0.06 (n = 12)
<i>WAPCre<sup>c</sup></i>	Nulliparous (d44)	End bud/duct	90.73 $\pm$ 0.02 (n = 12)
	1st pregnancy	Alveoli	96.80 $\pm$ 0.02 (n = 24)

<sup>a</sup> SE, standard error.

latency suggests that the internally truncated mutant p53 protein expressed under the endogenous promoter might not work in a dominant-negative manner.

Mammary tumors in all groups of mice are heterogeneous including adenocarcinoma, myoepithelial adenocarcinoma, adenosquamous carcinoma, and spindle cell tumor (Fig. 4, A-D). The majority of tumors were poorly differentiated invasive adenocarcinomas that share the most histopathological similarity with human tumors. In addition to mammary tumors, a few *p53<sup>flp/flp</sup>MMTVCre<sup>a</sup>* mice also developed lymphoma caused by a very low level of Cre activity in the lymphocytes or a low spontaneous incidence in aged C57BL/6  $\times$  129sv mice. On the other hand, other tumor types were found in *p53<sup>flp/flp</sup>MMTVCre<sup>b</sup>* and *p53<sup>flp/flp</sup>WAPCre<sup>c</sup>* mice caused by a broader Cre expression pattern (Table 2; Fig. 2A).

Importantly, up to half of *p53<sup>flp/flp</sup>MMTVCre<sup>a</sup>* mice had mammary tumor metastasis either in lung and/or liver after gross examination (Table 2; Fig. 4, E and F). Metastatic mammary tumor foci were also detected in *p53<sup>flp/flp</sup>MMTVCre<sup>b</sup>* and *p53<sup>flp/flp</sup>WAPCre<sup>c</sup>* mice (Table 2).

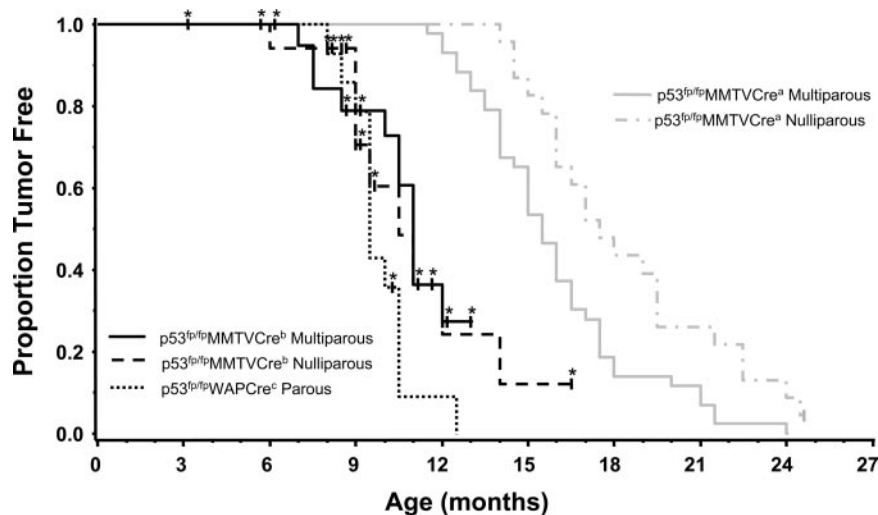
**Molecular Characterization of Mammary Tumors.** Estrogen is critical in the etiology of breast cancer and ER $\alpha$  mediates estrogen

responsiveness in breast cancer. Significantly, 40% of the *p53<sup>flp/flp</sup>WAPCre<sup>c</sup>* mice (n = 15) had both ER $\alpha$ - and PR-positive tumors (Fig. 4H), compared with 42 tumors from *p53<sup>flp/flp</sup>MMTVCre* mice that were all ER $\alpha$ - and PR-negative (Fig. 4G). The percentage of ER $\alpha$ -positive cells in ER $\alpha$ -positive tumors is over 90% whereas in ER $\alpha$ -negative tumors, no ER $\alpha$ -positive tumor cells were seen. The expression of ER $\alpha$  in tumors from *p53<sup>flp/flp</sup>WAPCre<sup>c</sup>* but not *p53<sup>flp/flp</sup>MMTVCre* mice was further confirmed by Western blotting analysis (Fig. 4L). In contrast to ER $\alpha$ , ER $\beta$  was expressed in all tumors (Fig. 4L and data not shown). The closely correlated expression of ER $\alpha$  and PR, a downstream target of ER, suggests that ER $\alpha$  is functional in ER $\alpha$ -positive tumors. To further test this notion, adenoviruses carrying green fluorescent protein regulated by estrogen-response elements (EREs; 32) were used to infect tumor cells prepared from *p53<sup>flp/flp</sup>MMTVCre* and *p53<sup>flp/flp</sup>WAPCre<sup>c</sup>* mice. After treatment with estradiol, green fluorescent protein-positive cells were detected in tumor cells from *p53<sup>flp/flp</sup>WAPCre<sup>c</sup>* but not *p53<sup>flp/flp</sup>MMTVCre* mice (Fig. 4M). Thus, ER $\alpha$  in the ER $\alpha$ -positive *p53<sup>flp/flp</sup>WAPCre<sup>c</sup>* tumors is transcriptionally active.

Deregulation of ER $\alpha$  expression during the premalignant stages of human breast carcinogenesis has been reported (33). Correspondingly, an increase of ER $\alpha$ -positive cells as well as clusters of ER $\alpha$ -positive cells in the normal gland, was observed in mammary intraepithelial neoplasia (34) but not in hyperplasia without atypia (Fig. 4I). Thus, similar to human breast cancer, there are multistep histopathological changes and alterations in the ER $\alpha$  expression pattern during the progression of mammary carcinogenesis in these models.

Frequent genetic changes and prognostic markers of human breast cancer have been identified. To test whether this mouse model parallels human breast cancer in these alterations, selected genes were

Fig. 3. Tumor-free survival curves in *p53<sup>flp/flp</sup>; Cre* mice. Survival curves were computed using the Kaplan-Meier product-limit method and compared using the generalized Wilcoxon statistic. Animals sacrificed before development of a mammary tumor are censored at the time of sacrifice and are shown with vertical tick marks plus asters. The numbers of mice are as follows: nulliparous *p53<sup>flp/flp</sup>MMTVCre<sup>a</sup>* (n = 23); multiparous *p53<sup>flp/flp</sup>MMTVCre<sup>a</sup>* (n = 43); nulliparous *p53<sup>flp/flp</sup>MMTVCre<sup>b</sup>* (n = 19); multiparous *p53<sup>flp/flp</sup>MMTVCre<sup>b</sup>* (n = 20); and parous *p53<sup>flp/flp</sup>WAPCre<sup>c</sup>* (n = 14).

Table 2 Tumor formation in *p53<sup>flp/flp</sup>; Cre* mice

<i>Cre</i> transgene	<i>MMTVCre<sup>a</sup></i> (Nulliparous)	<i>MMTVCre<sup>a</sup></i> (Multiparous)	<i>MMTVCre<sup>b</sup></i> (Nulliparous)	<i>MMTVCre<sup>b</sup></i> (Multiparous)	<i>WAPCre<sup>c</sup></i> (Parous)
Total number of mice	14	37	19	20	12
Mammary tumor	14 (100%)	37 (100%)	9 (47%)	12 (60%)	11 (92%)
Lymphoma	2 (14%)	6 (16%)	15 (79%)	15 (75%)	5 (42%)
Other tumor types <sup>a</sup>	— <sup>c</sup>	—	—	—	2 (17%)
Metastasis <sup>b</sup>	7 (50%)	13 (35%)	1 of 3 (33%), IC <sup>d</sup>	1 of 4 (25%), IC	4 (36%)
Multiple mammary tumors	11 (79%)	22 (59%)	3 of 4 (75%), IC	7 of 10 (70%), IC	8 (67%)
Median tumor latency (months)	17.5	15.5	10.5	11	9.5

<sup>a</sup> Other tumor types, such as soft tissue tumors.

<sup>b</sup> The number of mammary tumor bearing-mice had metastasis of mammary tumor origin.

<sup>c</sup> —, not detected.

<sup>d</sup> IC, incomplete.

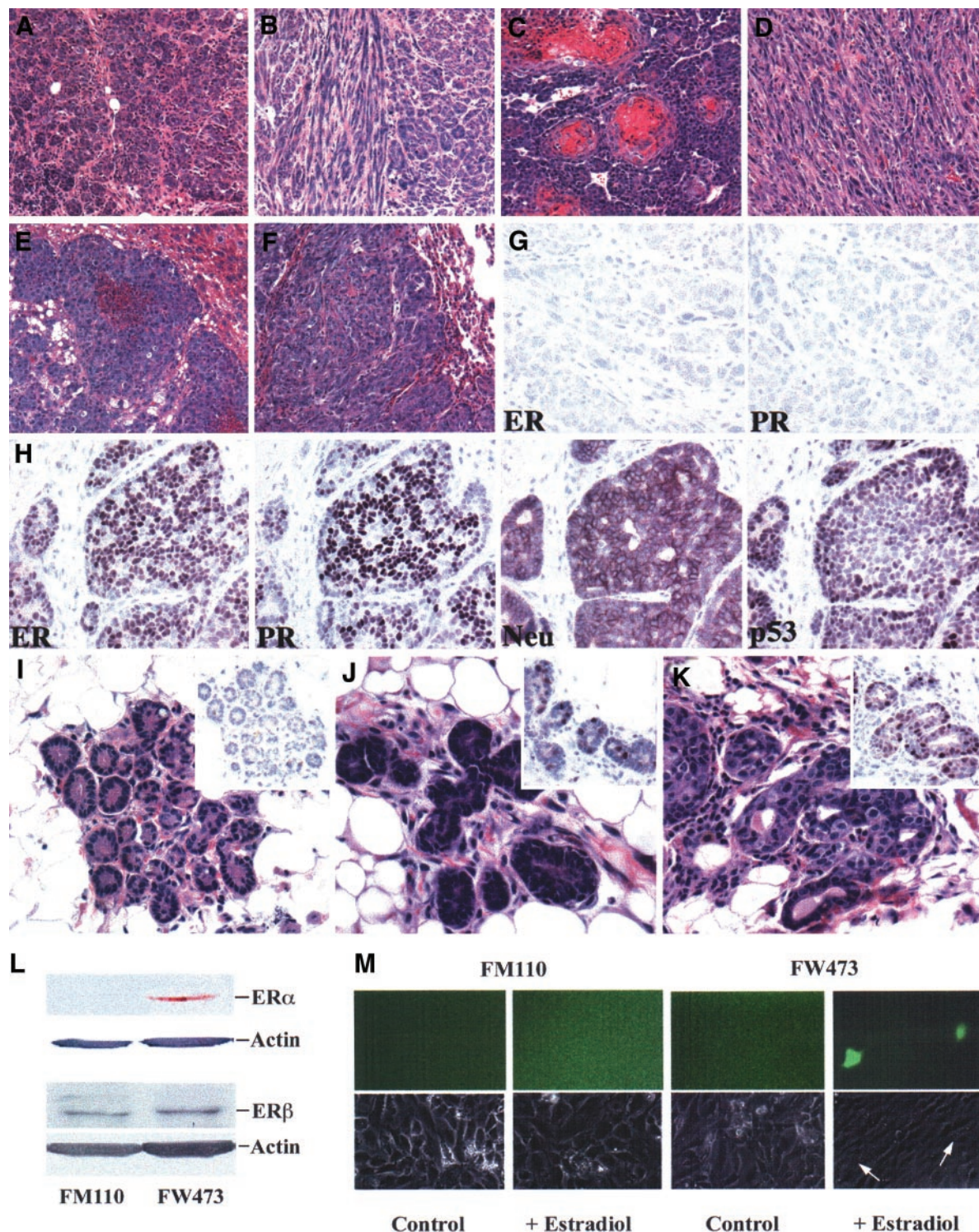


Fig. 4. Histological characterization of mammary tumors. Primary mammary tumors from *p53<sup>fl/fl</sup>; Cre* mice showed various histological features, including adenocarcinoma (A), myoepithelial adenocarcinoma (B), squamous cell carcinoma (C), and spindle cell tumor (D). Metastatic mammary tumors in the liver (E) and lung (F). Immunophenotypes of mammary tumors showing estrogen receptor  $\alpha$  (ER $\alpha$ )- and PR-negative staining (G), and ER $\alpha$ -, PR-, Neu-, and p53-positive staining (H). I-K, premalignant lesions of mammary gland. I, hyperplasia without atypia with negligible ER $\alpha$  expression (inset). J-K, mammary intraepithelial neoplasia (MIN) with increased ER $\alpha$  expression (inset). L, Western analysis of ER $\alpha$  and ER $\beta$  expression in tumors from *p53<sup>fl/fl</sup>MMTVCre<sup>+</sup>* (FM110) and *p53<sup>fl/fl</sup>WAPCre<sup>c</sup>* (FW473) mice. M, estrogen and estrogen receptor responsiveness of tumor cells. Fluorescence microscopy analysis of ER $\alpha$ -negative tumor cells (FM110) and of ER $\alpha$ -positive tumor cells (FW473) infected with Ad-25ERE-GFP in the presence or absence of estradiol. Original magnifications,  $\times 200$  (A-F) and  $\times 400$  (G-K).

examined (Fig. 5). Amplification or overexpression of *c-myc* proto-oncogene is frequently observed in human breast cancer (35). In this model, *c-myc* amplification is found in  $\sim 35\%$  of mammary tumors from *p53<sup>fl/fl</sup>MMTVCre* mice (Fig. 5A). About two-thirds of tumors from *p53<sup>fl/fl</sup>MMTVCre* and *p53<sup>fl/fl</sup>WAPCre<sup>c</sup>* mice showed Neu/

erbB2 overexpression by immunostaining and Western blot analysis using anti-Neu/erbB2 and phosphotyrosine antibodies (Figs. 4H and 5B). Overexpressed Neu/erbB2 appears to be active because tyrosine residues of the receptors are phosphorylated (Fig. 5B). In addition, the activity of matrix metalloproteinase (MMP), matrix metalloproteinase

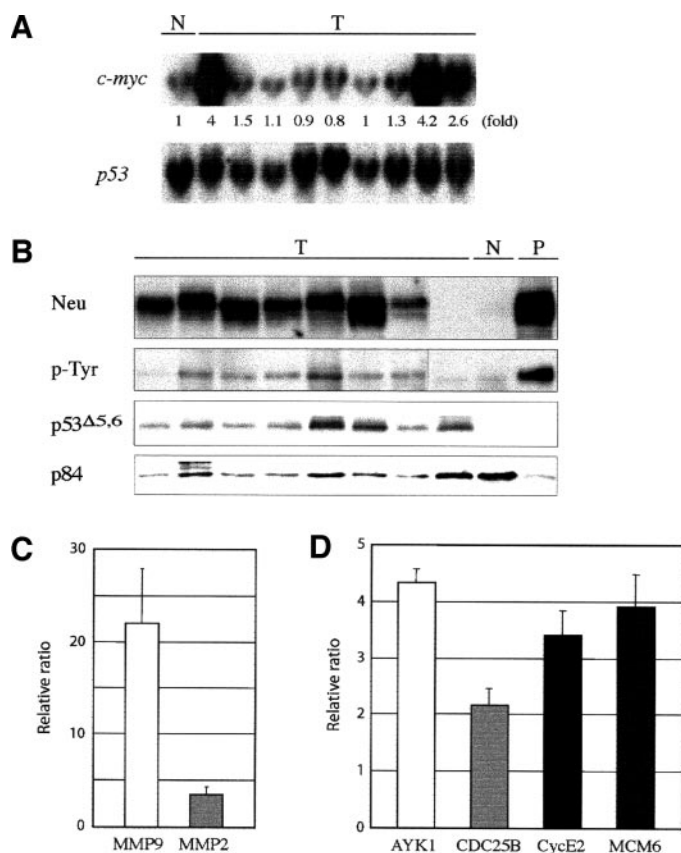


Fig. 5. Molecular characterization of mammary tumors. **A**, Southern blotting analysis of *c-myc* amplification in mammary tumors. The gene from which each probe is derived is given at left. The number between top and bottom blots indicates the relative intensity of *c-myc* signal (fold) of tumors (*T*) compared with the normal control sample (*N*) after normalized with the intensity of *p53* signal. **B**, Western analysis of erbB2 levels using anti-erbB2 (Neu) and phosphotyrosine (p-Tyr) antibodies, truncated *p53* protein (*p53* $\Delta$ 5,6), and a loading control (p84). *T*, mammary tumors; *N*, normal mammary gland control; *P*, mammary tumor from an *MMTV-Neu*-transgenic mouse. **C**, changes in the relative activity of matrix metalloproteinase 9 (MMP9) and MMP2 in mammary tumors assayed by gelatin zymography. The value was normalized as a ratio to the activity of normal mammary gland. **D**, changes in the expression of several prognostic markers in mammary tumors. The relative levels of mRNAs of AYK1, CDC25B, cyclin E2, and MCM6 were analyzed by reverse transcription-PCR. Each value was normalized using the amount of ribosomal protein S16 reverse transcription-PCR product and was expressed as a ratio to the amount of mRNA in normal mammary gland.

9 but not matrix metalloproteinase 2, was increased dramatically (Fig. 5C). Several prognostic markers [e.g., AYK1 (STK15), CDC25B, cyclin E2, and MCM6] identified recently through gene expression profiling in human breast cancer (36, 37) also showed enhanced expression in these tumors (Fig. 5D).

## DISCUSSION

Mice in a C57BL/6  $\times$  129sv background are normally resistant to mammary tumor development (38, 39), but loss of *p53* leads to a nearly complete incidence of mammary tumor with a high rate of metastasis to lung or liver. As the number of *p53*-inactivated cells increases, the MTL shortens. MTL reaches a plateau when  $\geq 20\%$  of the cells are targeted, indicating that there is a limit to the rate of breast carcinogenesis. Because ER $\alpha$ -positive mammary tumors develop in prepubertal/pubertal but not in adult mice, the timing of *p53* inactivation might be critical for determining ER $\alpha$  expression. Genetic changes (e.g., in *c-myc* and Her2/Neu/erbB2) and prognostic markers [e.g., AYK1 (STK15), CDC25B, cyclin E2, and MCM6] associated with human breast cancer are also seen in these mouse tumors.

Despite the use of different promoters with Cre, both luminal epithelial

and myoepithelial cells were targeted by Cre recombinase, as indicated by the *Rosa26* reporter strain (29). Heterogeneous tumor types (adenocarcinomas, myoepithelial adenocarcinomas, adenosquamous carcinomas, and spindle cell tumors) were seen in all mouse strains (Fig. 4). The majority of tumors were poorly differentiated invasive adenocarcinomas, which were also the most similar to human tumors histopathologically. Nonmammary tumors were also found, probably attributable to Cre expression in other tissues (Table 2; Fig. 2A). About 50% of mammary tumors metastasize to lung or liver (Table 2). Both histopathology and microarray analyses (data not shown) support that lung lesions are indeed tumor metastases. The metastasis frequency correlated with neither specific Cre-transgenic line nor tumor latency, consistent with previous observations (40). This tumor system recapitulates the high frequency of metastasis seen in advanced human breast cancer. By contrast, the experience of some investigators indicated that most mouse tumor models represent an early nonmetastatic stage of tumor development (41). Lung metastasis was also found in *p53* $^{-/-}$ -BALB/c mammary gland transplant models (42); however, the precise metastasis rate is not clear.

These mouse mammary tumors exhibit a pattern of mutation and gene dysregulation similar to human breast cancer. Amplification or overexpression of the *c-myc* and *erbB2* proto-oncogenes is frequently observed in human breast cancer (7, 35). About 35% of these mammary tumors were found to have *c-myc* amplification and two-thirds showed erbB2 overexpression. Matrix metalloproteinase 9 and cell cycle regulators such as AYK1 (STK15), CDC25B, cyclin E2, and MCM6 were up-regulated in these tumor cells. This is consistent with the recent results showing that overexpression of these genes in human breast cancer reflects poor prognosis (36, 37). The high frequencies of *c-myc* amplification and overexpression of erbB2 and cell cycle regulators in *p53*-mutated tumors suggest that these genetic alterations have pivotal roles during tumor progression.

An inverse relationship between the number of targeted cells and MTL was observed. It is reasonable to assume that larger numbers of targeted cells are more likely to acquire critical genetic changes leading to tumor development with shorter latency. Indeed, similar genetic (e.g., *c-myc*) and gene expression changes (e.g., Neu/erbB2, AYK1, CDC25B, cyclin E2, and MCM6) were seen at high frequencies in tumors of both short and long latency. Intriguingly, when the number of targeted cells exceeded 20%, MTL did not shorten further. To explain this phenomena, we assume that cancer initiation depends in part on the accumulation of a certain number of key mutations (43). If the key rate-limiting process was simply the accumulation of one additional mutation, then after the average cell has gone through *T* rounds of cell division, the probability of obtaining the key mutation is  $NuT$ , where *N* is the number of target cells with the predisposing mutation and *u* is the mutation rate per cell division. If there are two rate-limiting mutational steps, then the probability of obtaining both mutations is, from the gamma distribution, approximately  $N(uT)^2/2$ . If we suppose *u* is approximately  $10^{-6}$ , and there are about *T* = 10 rounds of cell division, then saturation would happen when *N* is of the order  $10^{10}$ , which is probably much higher than the actual number of cells at saturation. Thus, to explain the saturation kinetics, there are two alternatives. First, the mutation rate per cell division may be higher than  $10^{-6}$ . This may occur because mutations of *p53* increase the mutation rate per cell division. Second, some precancerous clonal expansion may be occurring, which would increase the number of rounds of cell division and therefore decrease the number *N* of initial predisposing target cells needed to achieve saturation. On the basis of results of the *MMTVCre<sup>b</sup>* line, it can be concluded that a saturation kinetic is reached by targeting  $\sim 20\%$  of mouse mammary epithelial cells. In the *WAPCre<sup>c</sup>* line, it is likely that a different population of mammary epithelial cells is targeted; however, the tumor kinetics is similar to that of *MMTVCre<sup>b</sup>*. In addition to the number of targeted

cells, it is plausible that the tumor latency might also be reflective of the type of cells targeted. Because multiple cell types are targeted in the models described here, the contribution of cell numbers and types of cells cannot be clearly differentiated.

On the basis of microarray profiling analysis, human breast cancers can be classified into five subtypes (44). It is not clear whether these heterogeneous tumor types are originated from different cells of the mammary gland or specific cancer-initiating cells are targeted and heterogeneity develops subsequently during tumor progression. Recent studies have revealed that a population of breast cancer cells possess stem cell-like properties (45). However, it remains to be studied whether cancer-initiating cells of ER $\alpha$ -positive and -negative tumors are different. In *WAPCre<sup>c</sup>* mice both ER $\alpha$ -positive and -negative mammary tumors were found, although mutations of *p53* in *MMTVCre* mice resulted in only ER $\alpha$ -negative tumors. Parity may not be relevant because ER $\alpha$ -positive tumors were found in both nulliparous and parous *p53<sup>flp/flp</sup>WAPCre<sup>c</sup>* mice. It is plausible that ER $\alpha$ -positive stem cells, in addition to ER $\alpha$ -negative stem cells, are targeted in *WAPCre<sup>c</sup>* mice. In contrast, in *MMTVCre* mice, only ER $\alpha$ -negative stem cells are targeted. Because nearly 90% of cells are LacZ-positive during second pregnancy in *MMTVCre* mice (data not shown), this might suggest that only a small population of cells give rise to ER $\alpha$ -positive tumors in these adult parous mice. The Cre transgenes are active at different developmental stages in *WAPCre<sup>c</sup>* and *MMTVCre* mice. Whether developmental stages affect the abundance of ER $\alpha$ -positive progenitor cells is not clear. Because it is feasible to isolate ER $\alpha$ -positive epithelial cells from normal mammary glands and tumors (32),<sup>8</sup> molecular mechanisms underlying ER $\alpha$ -positive and -negative mammary carcinogenesis can be systematically addressed using this model.

## ACKNOWLEDGMENTS

We thank Drs. Frank Graham and Lawrence Chan for Cre adenoviruses, Jolene Windle for the plasmid pBSpKCR3, Kornelia Polyak for Ad-25ERE-GFP viruses, Robert Reddick for histopathological comments, and Steve Lipkin and Paul Wakenight for critical review of the manuscript. We appreciate the contribution of Dr. Nanping Hu in the early phase of the project and of Kathryn Bushnell, Meihua Song and Elvira Gerbino for technical support. This work was initiated at the University of Texas Health Science Center at San Antonio.

## REFERENCES

- Bieche I, Lidereau R. Genetic alterations in breast cancer. *Genes Chromosomes Cancer* 1995;14:227–51.
- Hollstein M, Hergenhahn M, Yang Q, Bartsch H, Wang ZQ, Hainaut P. New approaches to understanding p53 gene tumor mutation spectra. *Mutat Res* 1999;431:199–209.
- Malkin D. Germline p53 mutations and heritable cancer. *Annu Rev Genet* 1994;28:443–65.
- Hahn WC, Weinberg RA. Modelling the molecular circuitry of cancer. *Nat Rev Cancer* 2002;2:331–41.
- Sharpless NE, DePinho RA. p53: good cop/bad cop. *Cell* 2002;110:9–12.
- Vogelstein B, Lane D, Levine AJ. Surfing the p53 network. *Nature (Lond)* 2000;408:307–10.
- Brisson O. Gene amplification and tumor progression. *Biochim Biophys Acta* 1993;1155:25–41.
- Donehower LA, Harvey M, Slagle BL, McArthur MJ, Montgomery CA, Butel J, Bradley A. Mice deficient for p53 are developmentally normal but susceptible to spontaneous tumours. *Nature (Lond)* 1992;356:215–21.
- Jacks T, Remington L, Williams BO, et al. Tumor spectrum analysis in p53-mutant mice. *Curr Biol* 1994;4:1–7.
- Harvey M, McArthur MJ, Montgomery CA Jr, Butel JS, Bradley A, Donehower LA. Spontaneous and carcinogen-induced tumorigenesis in p53-deficient mice [see comments]. *Nat Genet* 1993;5:225–9.
- Jerry DJ, Kittrell FS, Kuperwasser C, et al. A mammary-specific model demonstrates the role of the p53 tumor suppressor gene in tumor development. *Oncogene* 2000;19:1052–8.
- Jonkers J, Meuwissen R, van der Gulden H, Peterse H, van der Valk M, Berns A. Synergistic tumor suppressor activity of BRCA2 and p53 in a conditional mouse model for breast cancer. *Nat Genet* 2001;29:418–25.
- Anderson E. The role of oestrogen and progesterone receptors in human mammary development and tumorigenesis. *Breast Cancer Res* 2002;4:197–201.
- Masood S. Estrogen and progesterone receptors in cytology: a comprehensive review. *Diagn Cytopathol* 1992;8:475–91.
- Trichopoulos D, MacMahon B, Cole P. Menopause and breast cancer risk. *J Natl Cancer Inst (Bethesda)* 1972;48:605–13.
- Nandi S, Guzman RC, Yang J. Hormones and mammary carcinogenesis in mice, rats, and humans: a unifying hypothesis. *Proc Natl Acad Sci USA* 1995;92:3650–7.
- Yoshidome K, Shibata MA, Coudrey C, Korach KS, Green JE. Estrogen promotes mammary tumor development in C3(1)/SV40 large T-antigen transgenic mice: paradoxical loss of estrogen receptor alpha expression during tumor progression. *Cancer Res* 2000;60:6901–10.
- Brodie SG, Xu X, Qiao W, Li WM, Cao L, Deng CX. Multiple genetic changes are associated with mammary tumorigenesis in Brca1 conditional knockout mice. *Oncogene* 2001;20:7514–23.
- Ludwig T, Fisher P, Ganesan S, Efstratiadis A. Tumorigenesis in mice carrying a truncating Brca1 mutation. *Genes Dev* 2001;15:1188–93.
- Ludwig T, Fisher P, Murty V, Efstratiadis A. Development of mammary adenocarcinomas by tissue-specific knockout of Brca2 in mice. *Oncogene* 2001;20:3937–48.
- Parker B, Sukumar S. Distant metastasis in breast cancer: molecular mechanisms and therapeutic targets. *Cancer Biol Ther* 2003;2:14–21.
- Greenberg PA, Hortobagyi GN, Smith TL, Ziegler LD, Frye DK, Buzdar AU. Long-term follow-up of patients with complete remission following combination chemotherapy for metastatic breast cancer. *J Clin Oncol* 1996;14:2197–205.
- Stambolic V, Tsao MS, Macpherson D, Suzuki A, Chapman WB, Mak TW. High incidence of breast and endometrial neoplasia resembling human Cowden syndrome in *pten<sup>-/-</sup>* mice. *Cancer Res* 2000;60:3605–11.
- Pattengale PK, Stewart TA, Leder A, et al. Animal models of human disease. Pathology and molecular biology of spontaneous neoplasms occurring in transgenic mice carrying and expressing activated cellular oncogenes. *Am J Pathol* 1989;135:39–61.
- Guy CT, Cardiff RD, Muller WJ. Induction of mammary tumors by expression of polyomavirus middle T oncogene: a transgenic mouse model for metastatic disease. *Mol Cell Biol* 1992;12:954–61.
- Guy CT, Webster MA, Schaller M, Parsons TJ, Cardiff RD, Muller WJ. Expression of the neu protooncogene in the mammary epithelium of transgenic mice induces metastatic disease. *Proc Natl Acad Sci USA* 1992;89:10578–82.
- Lee EY, Chang CY, Hu N, et al. Mice deficient for Rb are nonviable and show defects in neurogenesis and haematopoiesis [see comments]. *Nature (Lond)* 1992;359:288–94.
- Howes KA, Ransom N, Papermaster DS, Lasudry JG, Albert DM, Windle JJ. Apoptosis or retinoblastoma: alternative fates of photoreceptors expressing the HPV-16 E7 gene in the presence or absence of p53 [published erratum appears in *Genes Dev* 1994;8:1738]. *Genes Dev* 1994;8:1300–10.
- Soriano P. Generalized lacZ expression with the ROSA26 Cre reporter strain [letter]. *Nat Genet* 1999;21:70–1.
- Wagner KU, McAllister K, Ward T, Davis B, Wiseman R, Hennighausen L. Spatial and temporal expression of the Cre gene under the control of the MMTV-LTR in different lines of transgenic mice. *Transgenic Res* 2001;10:545–53.
- Utomo AR, Nikitin AY, Lee WH. Temporal, spatial, and cell type-specific control of Cre-mediated DNA recombination in transgenic mice. *Nat Biotechnol* 1999;17:1091–6.
- Seth P, Porter D, Lahti-Domenici J, Geng Y, Richardson A, Polyak K. Cellular and molecular targets of estrogen in normal human breast tissue. *Cancer Res* 2002;62:4540–4.
- Shoker BS, Jarvis C, Sibson DR, Walker C, Sloane JP. Oestrogen receptor expression in the normal and pre-cancerous breast. *J Pathol* 1999;188:237–44.
- Cardiff RD, Anver MR, Gusterson BA, et al. The mammary pathology of genetically engineered mice: the consensus report and recommendations from the Annapolis meeting [see comments]. *Oncogene* 2000;19:968–88.
- Liao DJ, Dickson RB. c-Myc in breast cancer. *Endocr Relat Cancer* 2000;7:143–64.
- Perou CM, Sorlie T, Eisen MB, et al. Molecular portraits of human breast tumours. *Nature (Lond)* 2000;406:747–52.
- van 't Veer LJ, Dai H, van de Vijver MJ, et al. Gene expression profiling predicts clinical outcome of breast cancer. *Nature (Lond)* 2002;415:530–6.
- Ullrich RL, Bowles ND, Satterfield LC, Davis CM. Strain-dependent susceptibility to radiation-induced mammary cancer is a result of differences in epithelial cell sensitivity to transformation. *Radiat Res* 1996;146:353–5.
- Medina D. Mammary tumorigenesis in chemical carcinogen-treated mice. I. Incidence in BALB-c and C57BL mice. *J Natl Cancer Inst (Bethesda)* 1974;53:213–21.
- Lifsted T, Le Voyer T, Williams M, et al. Identification of inbred mouse strains harboring genetic modifiers of mammary tumor age of onset and metastatic progression. *Int J Cancer* 1998;77:640–4.
- Van Dyke T, Jacks T. Cancer modeling in the modern era: progress and challenges. *Cell* 2002;108:135–44.
- Kuperwasser C, Hurlbut GD, Kittrell FS, et al. Development of spontaneous mammary tumors in BALB/c p53 heterozygous mice: a model for Li-Fraumeni syndrome. *Am J Pathol* 2000;157:2151–9.
- Knudson AG. Antioncogenes and human cancer. *Proc Natl Acad Sci USA* 1993;90:10914–21.
- Sorlie T, Perou CM, Tibshirani R, et al. Gene expression patterns of breast carcinomas distinguish tumor subclasses with clinical implications. *Proc Natl Acad Sci USA* 2001;98:10869–74.
- Al-Hajj M, Wicha MS, Benito-Hernandez A, Morrison SJ, Clarke MF. Prospective identification of tumorigenic breast cancer cells. *Proc Natl Acad Sci USA* 2003;100:3983–8.

<sup>8</sup> M. J. McArthur, C. A. Montgomery, J. Butel, A. Bradley, unpublished data.